IOP Conf. Series: Materials Science and Engineering **211** (2017) 012015 doi:10.1088/1757-899X/211/1/012015

Kalman filter implementation for small satellites using constraint GPS data

Elmahy M Wesam *, Xiang Zhang, Zhengliang Lu and Wenhe Liao

Nanjing University of Science and Technology, China

*Email: Wesam_elmahy@yahoo.com

Abstract. Due to the increased need for autonomy, an Extended Kalman Filter (EKF) has been designed to autonomously estimate the orbit using GPS data. A propagation step models the satellite dynamics as a two body with J_2 (second zonal effect) perturbations being suitable for orbits in altitudes higher than 600 km. An onboard GPS receiver provides continuous measurement inputs. The continuity of measurements decreases the errors of the orbit determination algorithm. Power restrictions are imposed on small satellites in general and nanosatellites in particular. In cubesats, the GPS is forced to be shut down most of the mission's life time. GPS is turned on when experiments like atmospheric ones are carried out and meter level accuracy for positioning is required. This accuracy can't be obtained by other autonomous sensors like magnetometer and sun sensor as they provide kilometer level accuracy. Through simulation using Matlab and satellite tool kit (STK) the position accuracy is analyzed after imposing constrained conditions suitable for small satellites and a very tight one suitable for nanosatellite missions.

1. Introduction

A Global Navigation Satellite System (GNSS) is a system comprising a constellation of satellites capable of providing accurate orbit determination (OD) and time synchronization. It transmits navigation signal required by GNSS users to estimate their Position, Velocity and Time (PVT) [1]. GPS consists of three segments: the control segment, the space segment and the user segment. User segment refers to the GPS receivers that use the satellite-transmitted signals for navigation [2]. The GPS space segment nominally consists of 24 satellites in six orbital planes they are designed to ensure a visibility of at least four satellites at all times. Only four satellites are needed for a navigation fix. The control segment consisting of worldwide ground stations to maintain the operation of the space segment. The system provides very precise positioning information in meter and cm level. The GPS offers an attractive alternative to ground-based tracking systems. It provides very comparable accuracy in an autonomous way or nearly autonomous as it depends on the GPS satellites. CubeSats have evolved from purely educational tools to a standard platform for technology demonstration and scientific instrumentation and application in less than a decade [3]. Due to their low cost in development, they are spreading widely and becoming the lead in the list of choices for satellite manufacturing. With the availability of light and low power receivers lead a direct way to the usage of GPS navigation in nanosatellites. In [4], it is found that 16 % of 94 studied pico- and nanosatellites carried a GPS receiver, not all have been successful. The CanX-2 nanosatellite was carrying a GPS receiver among other payloads. It provided promising results for GPS navigation on nanosats missions as it was the first mission to successfully deliver GPS

navigation fixes and raw measurements [5]. The measurements obtained from the GPS receiver can be applied for precise orbit determination (POD) in two ways either for post processing where a least squares technique is applied or in real- time onboard navigation where a Kalman filter is used [6]. An Extended Kalman Filter (EKF) is a filter suitable with nonlinear systems [8]. It allows for accurate prediction of a given state without requiring expansive past data to be stored and computed, which allows for efficient on-board computation. Accuracy at the decimeter level can only be achieved under the best cases: post processing dual-frequency data with continuous receiver operation providing accuracy in cm level [7]. Unfortunately, such requirements may not be accessible in nanosats as they have to operate with low power. Single-frequency receivers are more suitable for CubeSats. Several experiments especially atmospheric ones need very accurate positioning information in meter level to ensure their success. This high accuracy can not be accomplished using autonomous sensors like magnetometers and sun sensors as they provide kilometer level accuracy. The GPS accurate navigation information opens the door for more experiments to be carried onboard the CubeSat. This makes the nanosats perfect candidates for more experiments and challenges. As a result of these power restrictions, the GPS will be shut off most of the mission and open when performing experiments. In this paper, several constrained conditions are imposed on the availability of GPS data to see how this affects the corrected states accuracy. Thus, the remaining of current article is organized as follows: firstly, Section 2 outlines the OD process consisting of its three main parts (dynamical model, estimation technique and measurement model). Secondly, Section 3 shows the simulation scenario using simulated GPS measurements with different test cases and the results are also analyzed. Finally, Section 4 declares conclusions and future work.

2. The OD process using GPS data

To accomplish an OD process using GPS data a satellite orbit can be determined using a dynamical method of analysis, where a force model is used to represent the most effective forces acting on the satellite (depends on its altitude). With an initial state vector, the numerical integration of these accelerations will give the position of the satellites at discrete-time intervals, resulting in the so called predicted orbit. The dynamics then allow the propagation of the state forward in time. The GPS measurements and the dynamic information are combined through an EKF for the correction process and hence produce a GPS solution.

2.1. Satellite's Dynamic Model

For a continuous-time system, there are different forms for the state vector representation. Each form depends on the solution procedure and the analysis type. In this work, the position and velocity vectors, in the Earth Centered Inertial (ECI) coordinates frame, are used to represent the state. This form is more suitable for numerical processing and usually easier to deal with during the OD process since they have no singularities. The state is presented as Equation (1):

$$\mathbf{x}(t)=\begin{bmatrix}\mathbf{r}\\ \mathbf{v}\end{bmatrix}_{ECI}=\begin{bmatrix}x & y & z & \dot{x} & \dot{y} & \dot{z}\end{bmatrix}^T \tag{1}$$

The state dynamic model that describes its time changes. The state propagation is in Equation (2):

$$\begin{aligned}\dot{\mathbf{X}}(t)&=f(\mathbf{x}(t))+w(t)=\begin{bmatrix}\mathbf{v}(t)\\ a(t)\end{bmatrix}+w(t)\\ &=\begin{bmatrix}\dot{x} & \dot{y} & \dot{z} & a_x & a_y & a_z\end{bmatrix}^T+\begin{bmatrix}0 & 0 & 0 & w_x & w_y & w_z\end{bmatrix}^T\end{aligned} \tag{2}$$

The order of the total acceleration used in the current work is equal to Newton's acceleration and the acceleration perturbation due to J_2. The w terms represent the modeling errors arising from the limited acceleration order. The acceleration components, a_x , a_y and a_z are represented in the ECI frame, as Equation (3):

$$\begin{aligned} a_x &= a_{x_{Newton}} + a_{x_{J2}} = -\frac{\mu x}{r^3} + \frac{\mu J_2 R^2}{2}\left(15\frac{xz^2}{r^7} - 3\frac{x}{r^5}\right) \\ a_y &= a_{y_{Newton}} + a_{y_{J2}} = -\frac{\mu y}{r^3} + \frac{\mu J_2 R^2}{2}\left(15\frac{yz^2}{r^7} - 3\frac{y}{r^5}\right) \\ a_z &= a_{z_{Newton}} + a_{z_{J2}} = -\frac{\mu z}{r^3} + \frac{\mu J_2 R^2}{2}\left(15\frac{z^3}{r^7} - 9\frac{z}{r^5}\right) \end{aligned} \tag{3}$$

where: r is the norm vector between the center of the Earth and the satellite, the standard gravitational parameter $\mu = 3.986004418 * 10^{14}\ \ m^3 s^{-2}$, the dimensional coefficient $J_2 = 0.0010827$ has been found from satellite observations and the radius of the Earth $R = 6378.137\text{km}$ at the equator [9].

2.2. Continuous-Time EKF

The Kalman Filter (KF) is a recursive algorithm which requires only data from the last and current iterations as the predicted state estimate ($\hat{\mathbf{X}}_{k/k-1}$) contains all required information on the system up to time (k-1). The KF generates a new state estimate as new observations become available, thus opening the possibility of real-time estimation. In case of nonlinear systems, Extended Kalman Filter EKF is constructed by linearizing either the system equation or measurement equation or both about the current (predicted) state estimate. This is done using the first two terms of a Taylor series expansion and using the same structure of the linear Kalman filter to provide the next estimate [10]. This produces a constant term and a first derivative term, known as the Jacobian (a matrix of partial derivatives). Most physical systems are represented as continuous-time models while discrete-time measurements are frequently taken for state estimation via a digital processor. The filter is comprised of two main steps: the prediction and the update. In continuous–time form, the dynamics of a linear system (process and measurement models) can be represented by the following first-order vector-matrix differential shown in Equations (4) and (5):

$$\dot{\mathbf{x}}(t) = f(\mathbf{x}(t), \mathbf{u}(t)) + \mathbf{w}(t), \text{ and } \mathbf{w}(t) \sim N(0, \mathbf{Q}(t)) \tag{4}$$

$$\mathbf{z}(t) = h(\mathbf{x}(t)) + \mathbf{v}(t), \text{ and } \mathbf{v}(t) \sim N(0, \mathbf{R}(t)) \tag{5}$$

where as shown in Equation (6):

$$\mathbf{x}_k = \mathbf{x}(t_k), \hat{\mathbf{x}}_{0/0} = E[\mathbf{x}(t_0)], \mathbf{P}_{0/0} = \text{var}[\mathbf{x}(t_0)] \tag{6}$$

Suppose that as shown in Equation (7):

$$\phi(t) = \left.\frac{\partial f}{\partial x}\right|_{\hat{\mathbf{x}}(t), u(t)} \text{ and } \mathbf{H}_k = \left.\frac{\partial h}{\partial x}\right|_{\hat{\mathbf{x}}_{k/k-1}} \tag{7}$$

By solving Equations (8) and (9):

$$\dot{\hat{\mathbf{x}}}(t) = f\left(\hat{\mathbf{x}}(t), u(t)\right) \tag{8}$$

$$\dot{\mathbf{P}}(t) = \phi(t)\mathbf{P}(t) + \mathbf{P}(t)\phi^T(t) + \mathbf{Q}(t) \tag{9}$$

With Equation (10):

$$\hat{\mathbf{x}}(t_{k-1}) = \hat{\mathbf{x}}_{k/k-1} \text{ and } \mathbf{P}(t_{k-1}) = \mathbf{P}_{k/k-1} \tag{10}$$

The predicted state estimate and predicted covariance matrix will be as Equation (11):

$$\hat{\mathbf{x}}_{k/k-1} = \hat{\mathbf{x}}(t_k) \text{ and } \mathbf{P}_{k/k-1} = \mathbf{P}(t_k) \tag{11}$$

The update equations (12-16) of continuous-time EKF are identical to those of discrete-time EKF given by:

$$\boldsymbol{\Psi}_k = \mathbf{z}_k - \mathbf{h}\left(\hat{\mathbf{x}}_{k/k-1}\right) \tag{12}$$

$$\mathbf{S}_k = \mathbf{H}_k \mathbf{P}_{k/k-1} \mathbf{H}_k^T + \mathbf{R}_k \tag{13}$$

$$\mathbf{K}_k = \mathbf{P}_{k/k-1} \mathbf{H}_k^T \mathbf{S}_k^{-1} \tag{14}$$

$$\hat{\mathbf{x}}_{k/k} = \hat{\mathbf{x}}_{k/k-1} + K_k\ \boldsymbol{\Psi}_k \tag{15}$$

$$\mathbf{P}_{k/k} = (\mathbf{I} - K_k \mathbf{H}_k)\mathbf{P}_{k/k-1} \tag{16}$$

To prevent the Kalman filter divergence, the following algebraically equivalent covariance correction Equation (17), which is called "Joseph Alternative KF Form", is applied [10]:

$$\mathbf{P}_{k/k} = (\mathbf{I} - K_k \mathbf{H}_k)\mathbf{P}_{k/k-1}(\mathbf{I} - K_k \mathbf{H}_k)^T + K_k \mathbf{R}_k K_k^T \tag{17}$$

Where, the symmetry of matrix multiplication forces $P_{k/k}$ to remain symmetric. The first Jacobian state matrix, Φ, is independent of the type of measurement. Thus, Φ is given by Equation (18):

$$\Phi = \Phi\left(\hat{\mathbf{x}}(t)\right) = \begin{bmatrix} 0_{3x3} & I_{3x3} \\ \Phi_{33} & 0_{3x3} \end{bmatrix}_{\mathbf{x}(t)=\hat{\mathbf{x}}(t)} \quad and \ \ldots \ \Phi_{33} = \begin{bmatrix} \frac{\partial a_x}{\partial x} & \frac{\partial a_x}{\partial y} & \frac{\partial a_x}{\partial z} \\ \frac{\partial a_y}{\partial x} & \frac{\partial a_y}{\partial y} & \frac{\partial a_y}{\partial z} \\ \frac{\partial a_z}{\partial x} & \frac{\partial a_z}{\partial y} & \frac{\partial a_z}{\partial z} \end{bmatrix} \tag{18}$$

The partial derivatives are too lengthy to be stated here and are available in [11]. The Runge-Kutta method of fourth order is used to propagate the state and covariance in-between measurements. It provides good performance to a relatively low computational cost even for larger integration steps. The Kalman Filter can be "tuned" by adjusting the covariance of the process noise, w_k, and the covariance of the observation noise, v_k.

2.3. GPS measurement model

The atomic clocks aboard all GPS satellites are synchronized to a time referred to as GPS system time. GPS satellites continuously transmit signals that can be picked up by a GPS receiver. In an ideal case, 3 satellites are enough for a 3-dimensional position fix, but in practice a fourth satellite is needed to correct the receiver's clock as the receiver clock is not usually synchronized with the system time [12].
The vector **r** from the receiver to a GPS satellite can be expressed as Equation (19):

$$\mathbf{r} = \mathbf{S} - \mathbf{u} \tag{19}$$

where **S** is the position vector of the GPS satellite and **u** is the position vector of the receiver. The pseudo range p can be expressed as Equation (20):

$$p = r + c.t_u \tag{20}$$

c is the light's speed and t_u is the offset between receiver clock and GPS system time as Equation (21):

$$p - c.t_u = \|\mathbf{S} - \mathbf{u}\| \tag{21}$$

This is actually an equation for a sphere centered on the GPS satellite. We have a set of four unknowns (x_u, y_u, z_u, t_u): the receiver position and the time offset. With four satellites available, the pseudo range is as Equation (22):

$$p_i = \sqrt{(x_i - x_u)^2 + (y_i - y_u)^2 + (z_i - z_u)^2} + c.t_u \ , \ i=1:4 \tag{22}$$

where (x_i, y_i, z_i) are the individual GPS satellite positions.

The receiver velocity can be obtained by either forming an approximate derivative of the position or by studying the Doppler shift of the signal from individual satellites. More advanced techniques include using the carrier phase of the incoming signal to smooth the pseudo range obtained from the code phase to completely eliminate ionospheric error. The GPS receiver output is in the earth centered earth fixed (ECEF) frame. This fix information can be used to correct the on-board orbit propagator in the satellite, and it can also be downloaded from the satellite and used in more accurate orbit propagators. Satellite orbits are calculated in an earth centered inertial (ECI) frame as the equations of motion have to be applied in an inertial frame. The measured state vector is then transformed into ECI frame for compatibility. The observation Jacobian matrix, H is hence a 6x6 identity matrix [13].

3. Simulation scenario

Several scenarios are carried out with different constrained conditions to see the performance of the filter. The cases are tabulated in table.1 showing simulation times when the GPS receiver is on and off as well as the duty cycle. It has to be noted that the switching time differs from one mission to another depending on their own requirements. Case 5 in particular is suitable for nanosatellite operations.

3.1. The initial orbit and conditions for the EKF

A sun synchronous orbit (700 km) is chosen to test the filter so that the limited acceleration model outlined in the last section is convenient to be applied at that altitude. The reference state is generated from the high-precision orbit propagator (HPOP) in the satellite tool kit (STK). In the configuration, Runge-kutta 7/8 method for numerical integration of equations of motion, the EGM 96 model (up to a degree of 70*70) for perturbation due to the nonsymmetrical geopotential, Harris-Priester model for atmospheric drag, lunar/solar gravitational attraction and solar radiation pressure are also included. The atmospheric drag coefficient is set to 2.2, the solar radiation pressure coefficient is set to 1.0 and the constant area-to-mass ratio is set to 0.0043.

The initial state to start the filter is set as a truth model i.e. with no initial error. The simulated GPS measurements were created using the rand function in Matlab which produces normally distributed pseudo-random numbers, using a chosen error and rate. The error added to the position is 10 meters and to the velocity is 0.01. The Q and R are taken to be 6x6 diagonal matrices. The process noises for acceleration uncertainty are set to $1\text{x}10^{-5}$. The step size is 1 second and the initial covariance is set to:

$$\mathbf{P}_o = \text{diag}\left[(10\text{ m})^2, (10\text{ m})^2, (10\text{ m})^2, (0.01\text{m/s})^2, (0.01\text{m/s})^2, (0.01\text{m/s})^2\right]$$

R matrix is set to equal $\mathbf{P}_o$ as no initial error is present. When GPS measurements are not available, the solution is based only on the dynamics part, as it is better than not having a solution at all. This causes quick convergence when the measurements are available again. More details are in [7].

Table 1. Availability of GPS data.

Case #	GPS_ON	GPS_OFF	Duty cycle
Case 1	15 Min	15 Min	50 %
Case 2	10 Min	10 Min	50 %
Case 3	5 Min	15 Min	25 %

Case #	GPS_ON	GPS_OFF	Duty cycle
Case 4	5 Min	10 Min	25 %
Case 5	9.8 Min	88.2 Min	10 %
Case 6	-	-	100 %

Simulation results and analysis: The simulations were performed for 1 day, 8hours and 1 orbit to see how this affects the position error as well as to test the filter. After running simulations, the results are presented in table. 2 showing the average root sum square (ARSS) for position, the maximum RSS and the average root sum square AVSS for velocity.

Table 2. Simulation Results.

Case	ARSS [m]			Max RSS [m]			AVSS in [m/sec]		
	1 Day	8 h	1 Orb	1 Day	8 h	1 Orb	1 Day	8 h	1 Orb
Case 1	9.1904	8.1858	10.68	120.1	82.317	67.39	0.0313	0.0278	0.0339
Case 2	4.8439	4.209	4.822	55.114	39.8	41.739	0.0234	0.02	0.0244
Case 3	13.799	12.14	14.58	129.77	107.11	107.29	0.045	0.038	0.049
Case 4	8.2841	7.361	9.163	80.065	55.322	50.778	0.0347	0.0298	0.039
Case 5	348.72	378.51	542.9	1700.0	1340.0	1130.0	0.3569	0.3889	0.562
Case 6	0.5082	0.534	0.738	9.1657	8.823	9.683	0.0063	0.0063	0.0064

As expected, the position error increased as the time decreased. The difference in accuracy between Cases 1 and 2 is relatively high. Case 2 is better by nearly 50% in ARSS and the maximum RSS for all simulation times relative to case 1. Also, Cases 3 and 4 have a similar pattern. Different users maybe prefer one case to another depending on their requirements and what type of small satellite they have.

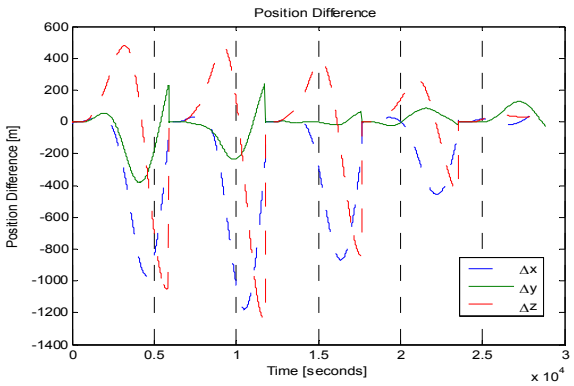

Figure 1. Position diff. 8h simulation Case 5.

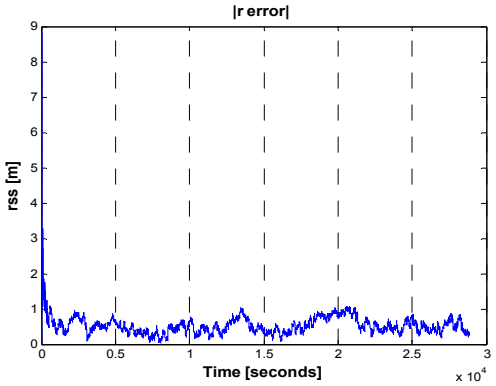

Figure 2. RSS 8h simulation Case 6.

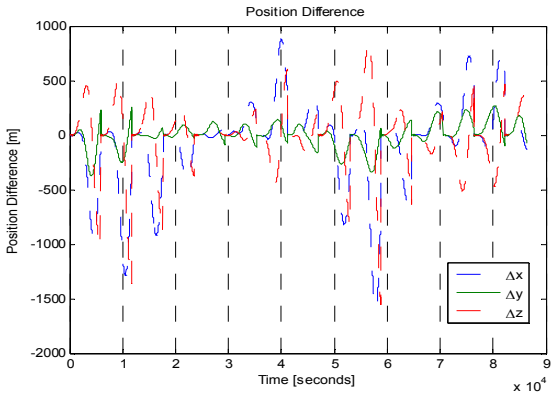

Figure 3. Pos. diff. 1 day simulation Case 5.

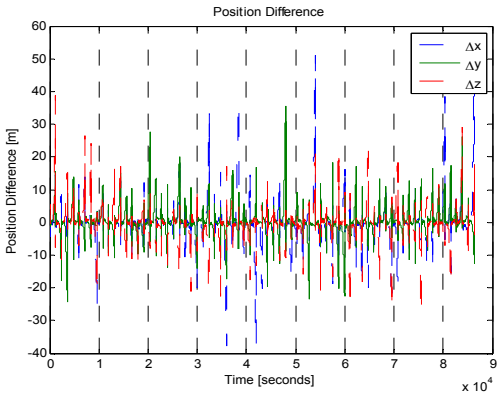

Figure 4. RSS 1 day simulation Case 2.

The microsatellites are more flexible than nanosatellites concerning the power limits making the cases other than Case 5 more suitable. Case 5 with the least duty cycle have the worst results of all cases which were also expected since saving power will result in less accurate results. The maximum error reaches 1.34km for 8h and 1.7km for 1 day simulation. This is still a very good result compared to the coarse accuracy provided by other sensors that can be onboard nanosatellites. Some values listed in table 2 are depicted for more clarity and to show the performance of the filter .Figures 1 and 2 show the position difference for Case 5 and the RSS for Case 6 with 8h simulation, respectively. Figures.3 and 4 show the 1 day simulation for Case 5 and Case 2, respectively.

4. Conclusion and future work

An EKF has been designed to autonomously correct the state using GPS measurements. The GPS measurements are simulated to represent only single-frequency data. Due to power constraints that are imposed on small satellites, especially nanosats, it is impossible for the GPS to be turned on all the time. In fact, in nanosats it will be shut down most of the mission's life time. For that reason, different test cases with different duty cycles and simulation times are applied. As expected, the accuracy degraded as the simulation time and the duty cycle decreased. On average ,a meter level is obtained even on a case with 10% duty cycle which is desirable when accurate on board tests are needed. For future work, more tuning for the filter is hopefully to be tried to reduce the maximum error. With real data available, it will be preferable to see the results in real case situation.

References

[1] Rush John 2000 Current issues in the use of the Global Positioning System aboard satellites *Acta Astronautica* **47** 2-9 pp 377-87
[2] Kaplan Elliott D and Christopher J Hegarty 2006 Understanding GPS: Principles and Applications Second Edition Artech House
[3] Puig-Suari J, Turner C and Twiggs R J 2001 CubeSat: The Development and Launch Support Infrastructure for Eighteen Different Satellite Customers on One Launch *Proceedings of AIAA/USU* Conf. Logan UT pp 1–5
[4] Bouwmeester J and J Guo 2010 Survey of worldwide pico- and nanosatellite missions, distributions and subsystem technology *Acta Astronautica 67* pp 854-62
[5] Kahr E, Montenbruck O, O'Keefe K, Skone S, et al 2011 GPS tracking on a nanosatellite CanX-2 flight experience *International ESA conference on guidance, navigation & control systems* (Karlovy Vary, Czech Republic) pp 5–10
[6] Oliver Montenbruck and Eberhard Gill 2005 Satellites Orbits Models Methods Applications (3rd Edition, Springer Berlin, Heidelberg, NewYork)
[7] Mander, Amandeep 2011 *Constrained GPS-based precise orbit determination of low earth orbiters* MSc. Thesis, York University
[8] Hendy H, Rui X T and Khalil M 2013 An Integrated GPS/INS Navigation System for Land Vehicle *Applied Mechanics and Materials* **336** pp 221-6
[9] D Vallado 2007 *Fundamentals of Astrodynamics and Applications* (3rd edition Springer, Hawthorne, CA)
[10] El-Mahy M K 1994 An Investigation into Kalman Filter Target Tracking Algorithms and their Real Time Parallel Transputer Implementation (Ph.D. Thesis Royal Military College of Science Cranfield University U.K)
[11] Rikard Ottemark 2015 Autonomous Satellite Orbit Determination Based on Magnetometer and Sun Sensor Measurements Design: Test and Verication (MSc. Thesis, Luleå University of Technology, Department of Computer Science, Electrical and Space Engineering)
[12] Hannu Leppinen 2013 Integration of a GPS subsystem into the Aalto-1 nanosatellite (MSc in Technology, School of Electrical Engineering Aalto University)
[13] Elizabeth M Keil 2014 Kalman Filter Implementation to Determine Orbit and Attitude of a Satellite in a Molniya Orbit *MSc in Aerospace and Ocean Engineering*

Acknowledgment

The research was supported by the Research Fund for the Doctoral Program of Higher Education of China (20113219110025). The authors declare that there is no conflict of interest regarding the publication of this paper.